Proceedings of the International Symposium on Engineering Lessons Learned from
the 2011 Great East Japan Earthquake, March 1-4, 2012, Tokyo, Japan

REAL-TIME DETECTION OF THE SOURCE AREA OF AN INTENSE TSUNAMI—CASE STUDY OF THE 2011 GREAT EAST JAPAN EARTHQUAKE

Yutaka HAYASHI[1], Hiroaki TSUSHIMA[2] and Yasuhiro YOSHIDA[3]

[1] Senior Researcher, Seismology and Volcanology Research Department, Meteorological Research Institute, Japan Meteorological Agency, Tsukuba, Japan, yhayashi@mri-jma.go.jp
[2] Researcher, Seismology and Volcanology Research Department, Meteorological Research Institute, Japan Meteorological Agency, Tsukuba, Japan, tsushima@mri-jma.go.jp
[3] Senior Researcher, Seismology and Volcanology Research Department, Meteorological Research Institute, Japan Meteorological Agency, Tsukuba, Japan, yyoshida@mri-jma.go.jp

ABSTRACT: Offshore tsunami waveform data from the 2011 Great East Japan earthquake indicate that the maximum-amplitude tsunami that struck the Tohoku district was of relatively short period. By comparing one seismic and two tsunami source models, we concluded that the short-period large-amplitude tsunami was generated within the area between the epicenter and the Japan Trench. We demonstrated that all three models are capable of real-time detection of future tsunami sources of similar intensity to that of the 2011 tsunami.

Key Words: Impulsive tsunami source, 2011 off the Pacific coast of Tohoku earthquake, strong-motion waveform inversion, tsunami back-propagation, tsunami waveform inversion

INTRODUCTION

A massive earthquake of moment magnitude (M_w) 9.0 occurred at 14:46 JST (05:46 UTC) on 11 March 2011, off the Pacific coast of northeastern Honshu, Japan. This earthquake, named the 2011 off the Pacific coast of Tohoku earthquake by the Japan Meteorological Agency (JMA; Hirose et al. 2011), is hereafter referred to as the 2011 Great East Japan earthquake. The epicenter was offshore, southeast of Sendai City (38°06.2′N, 142°51.6′E; JMA 2011). Only one previous earthquake of this seismic intensity (7, the upper limit of the JMA scale) has been observed since the JMA introduced instrument-based seismic intensity observations in 1996 (Hoshiba et al. 2010, 2011). Seismic intensities of 6-upper and 6-lower (JMA scale) were observed over an area of approximately 400 km × 100 km by many onshore seismic stations in the Tohoku and Kanto districts (Hoshiba et al. 2011).

The tsunami that accompanied the earthquake was detected offshore by coastal wave gauges (Nagai et al. 2005), real-time kinematic global positioning system (RTK-GPS) buoys (Kato et al. 2005), cabled deep ocean-bottom pressure gauges (OBPG) (e.g. Fujisawa et al. 1986; Hirata et al. 2002), and Deep-ocean Assessment and Reporting of Tsunamis (DART) buoys (González et al. 2005). In particular, OBPGs deployed off Tohoku recorded an impulsive tsunami of short period and large

amplitude (Ito et al. 2011). The periods of the initial tsunami waves observed off Hokkaido were longer than those observed off Tohoku. Thus, the most impulsive tsunami waves propagated westward from the source area.

In this paper, we compare tsunami source locations determined by a seismic fault model with slip distribution estimated by waveform inversion of strong ground motion (MODEL-1; Yoshida et al. 2011), by back-propagation of tsunami arrival times at offshore stations (MODEL-2; Hayashi et al. 2011), and from a deformation field determined by tsunami waveform inversion (MODEL-3; Tsushima et al. 2011). We then consider the real-time application of each modeling approach to the detection of intense tsunami sources such as that of the Great East Japan earthquake.

MODEL-1: STRONG-MOTION WAVEFORM INVERSION

Strong-motion data observed near an earthquake epicenter (< 500 km) can provide more detailed information about the source process of a large earthquake than can be obtained from teleseismic body

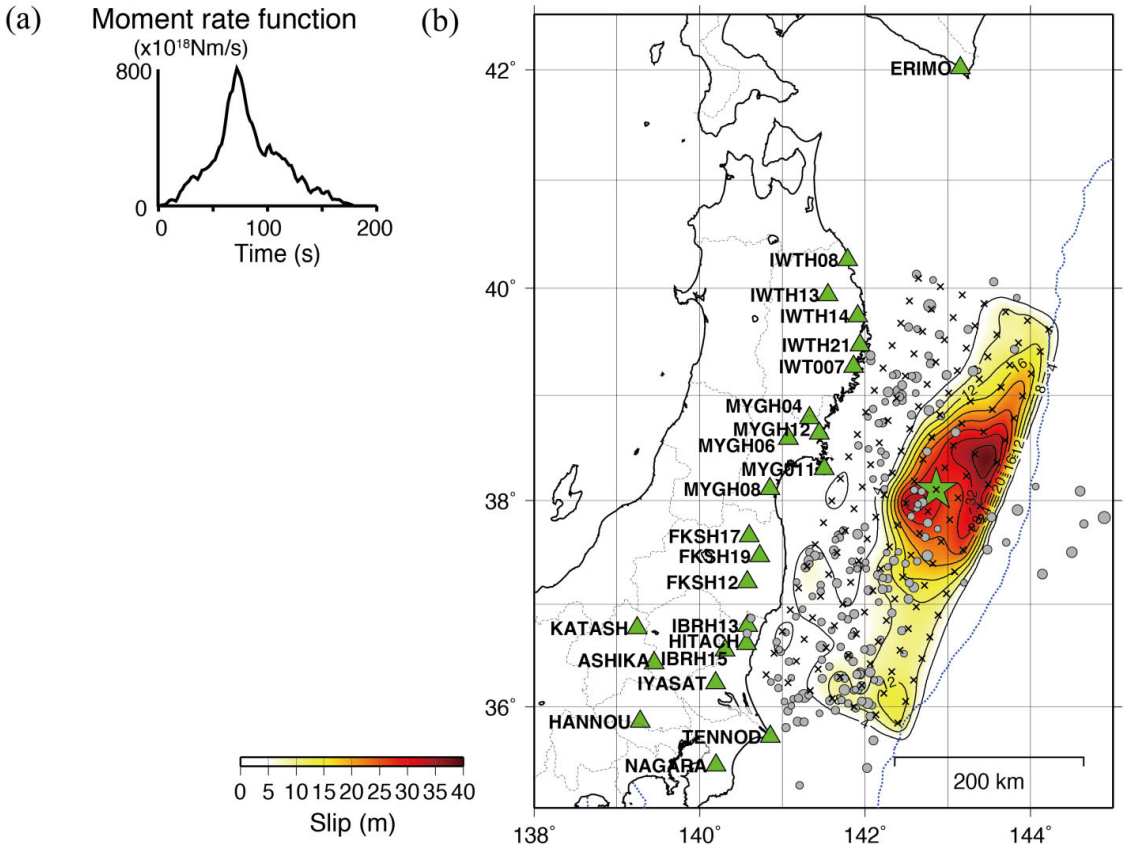

Fig. 1 Finite-source model of the 2011 Great East Japan earthquake from inversion of strong-motion waves (Yoshida et al. 2011). (a) Moment rate function. (b) Slip distribution on the fault. The large green star represents the epicenter of the main shock (M_w = 9.0); gray circles represent aftershocks ($M_{JMA} \geq 5.0$) within 24 h of the main shock. Crosses represent grid points on the fault plane used for calculation of synthetic waveforms. Triangles denote seismic stations used in this analysis. Slip distribution contour interval is 4 m. Twenty-three strong-motion seismograms were used from two K-NET stations (IWT007 and MYG011; Kinoshita 1998) and 13 KiK-net stations (IWTH08, IWTH13, IWTH14, IWTH21, MYGH04, MYGH12, MYGH06, MYGH08, FKSH17, FKSH19, FKSH12, IBRH13, and IBRH15; Aoi et al. 2000) deployed by the National Research Institute for Earth Science and Disaster Prevention (NIED) as well as eight stations from JMA (ERIMO, HITACH, IYASAT, KATASH, ASHIKA, HANNOU, TENNOD, and NAGARA).

wave data. Several studies have used strong-motion data to investigate the 2011 Great East Japan earthquake (e.g. Yoshida et al. 2011, Suzuki et al. 2011). Here, we summarize the results of strong-motion waveform inversion by Yoshida et al. (2011).

Twenty-three near-field strong-motion seismograms were used (Fig. 1). Acceleration seismograms were first integrated to velocity, then band-pass filtered (0.01–0.15 Hz) and decimated to 0.5 Hz. A time window of 250 s was used, starting from 10 s before the *P*-wave arrivals. Strike and dip of the fault plane were assumed to be 201° and 9°, respectively. The fault was assumed to measure 475 km along strike and 175 km in the dip direction. It was assumed that the rupture initiated at the hypocenter of the main shock determined by JMA. The fault plane was divided into sub-faults of 25 km × 25 km.

Green's functions were calculated for each sub-fault by the discrete wavenumber method (Bouchon 1981) using reflection–transmission matrices (Kennett and Kerry 1979). The inelasticity effect was accounted for by using a complex velocity field (Takeo 1985). The moment rate function for each sub-fault was expressed by 20 simple triangle functions of 8 s duration and overlapping by 4 s. The maximum rupture velocity was set at 2.5 km/s to minimize variance. The linear multiple time window inversion method was used with constraints on smoothness of the spatiotemporal slip distribution (e.g. Ide et al. 1996, Nakayama and Takeo 1997). Smoothness parameters (hyperparameters) were selected to minimize Akaike's Bayesian information criterion (ABIC) (Akaike 1980, Fukahata et al. 2003). Waveforms were aligned by onset time and weighted equally for all stations.

Fig. 1 shows the slip distribution obtained from the regional strong-motion data analysis. The total seismic moment was 3.4×10^{22} Nm ($M_w = 9.0$). The slip area extends eastward from the hypocenter to the shallowest part of the fault plane and maximum slip is 38 m. The fit between observed and synthetic waveforms is reasonably good, when a reduction in variance of the fitted model is assumed to be about 91%.

The sequence of released seismic moment is as follows. In the first stage of the rupture (0–40 s), the rupture expands radially outward from the hypocenter. In the next stage (40–80 s), the rupture area extends both north and south along the shallow part of the fault plane. The large amount of slip during this stage may have generated the impulsive tsunami. The rupture velocity is very slow (about 1 km/s) during the first and second stages. In the third stage (after 80 s), the rupture extends southward, reaching the southern end of the fault plane at 160 s.

MODEL-2: BACK-PROPAGATION OF TSUNAMI ARRIVAL TIMES

In this section, we summarize the estimation of the tsunami source area by back-propagation of tsunami arrival times by Hayashi et al. (2011).

The tsunami was detected at various offshore observation stations, including coastal wave gauges (Nagai et al. 2005), real-time kinematic global positioning system (RTK-GPS) buoys (Kato et al. 2005, cabled deep ocean-bottom pressure gauges (OBPG) (e.g. Fujisawa et al. 1986, Kanazawa and Hasegawa 1997, Hirata et al. 2002) Time-series of changes of sea-level and ocean-bottom pressure recorded following the 2011 Great East Japan earthquake were acquired from 21 observation stations (Figs. 2 and 3). Arrival times for each phase of the tsunami were manually read from waveforms (Fig. 2).

To define the edges of the tsunami source area, Huygens' Principle was applied to back-propagate the tsunami from each observation station. For these calculations tsunami travel-time software (TTT v. 3.0; Geoware in Hawaii, USA) was used with bathymetric data at 1 min intervals (ETOPO1; Amante and Eakins 2009). The phase velocity of tsunami propagation was assumed to be equal to the square root of gravity multiplied by water depth. For very large earthquakes, the time difference between the main shock and generation of the tsunami is not negligible (Seno and Hirata 2007). Therefore, for back-propagation from tsunami arrival times, time values were modified by 1 min / 120 km, corresponding to a distance from the epicenter to the contact point of the back-propagation curve with the tsunami source area (Fig. 3a). This correction was applied to account for differences between the time of the main shock and the generation of the tsunami and is equivalent to assuming an average

apparent (i.e. projected to the seafloor) fault rupture velocity of 2 km/s.

The tsunami source area determined by back-propagation of tsunami arrivals at offshore observation stations (Fig. 3a) was approximately 500 km long with a maximum width of about 200 km. The eastern edge of the source area was close to and approximately parallel to the western flank of the

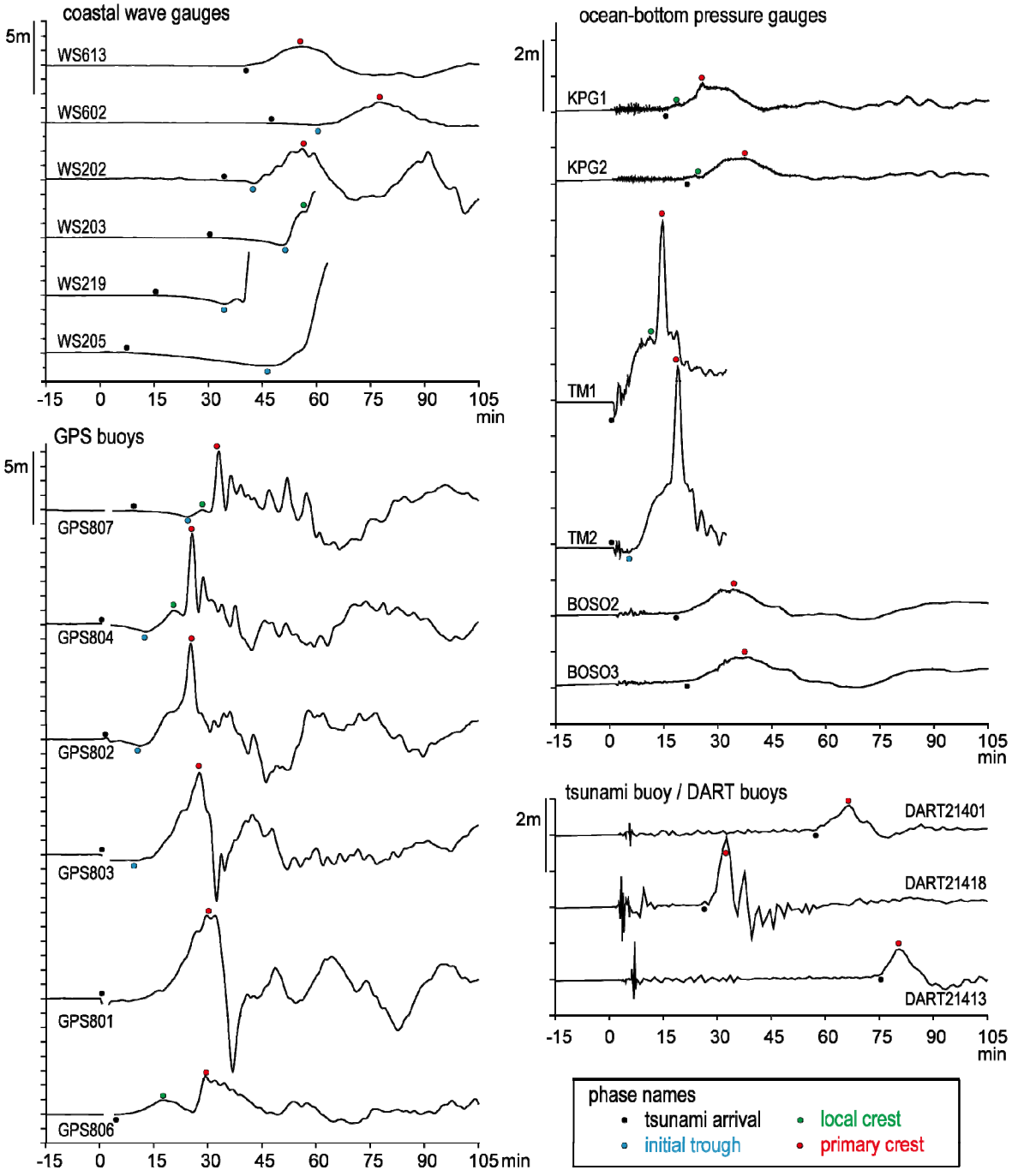

Fig. 2 Tsunami waveforms recorded offshore during and after the 2011 Great East Japan earthquake and phase nomenclature (Hayashi et al. 2011). Waveform data were low-pass filtered with cut-off period of 2 min. Online data transmission was interrupted at some observation stations, but data recovered afterwards are plotted. See Fig. 3 for locations of observation stations.

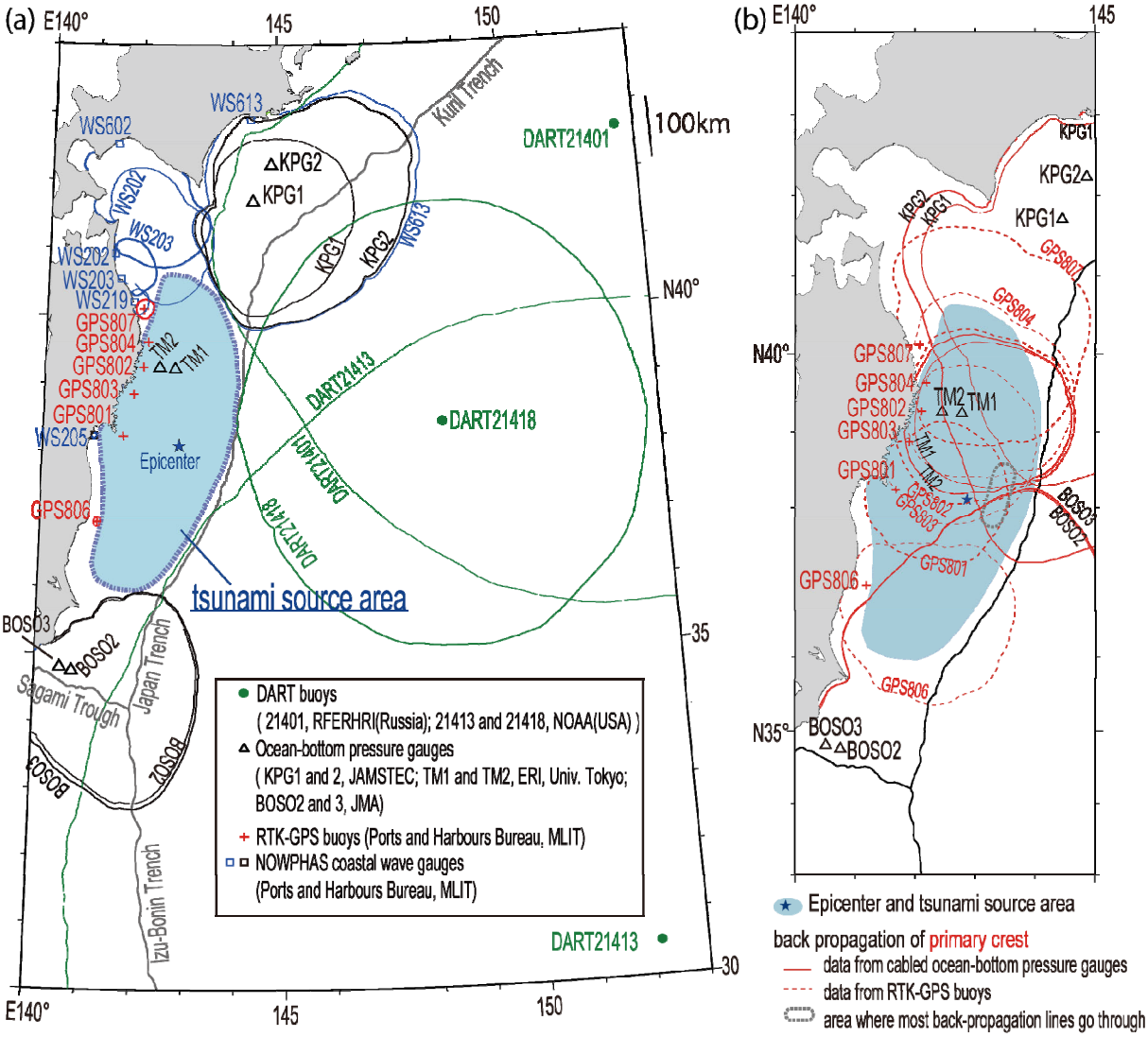

Fig. 3 Tsunami source area of the 2011 Tohoku earthquake determined by back-propagation of (a) tsunami arrivals and (b) arrival times of primary crests at offshore observation stations (Hayashi et al. 2011).

Japan Trench, and the southern edge was at about latitude 36°N. However, the aftershock area (Hirose et al. 2011) extended to the eastern side of the trench and farther south than the tsunami source area. Sea-level changes observed at stations TM1, TM2, GPS804, GPS802, GPS803, and GPS801 were almost synchronous with the arrival of the seismic wave, indicating that these offshore stations were within the tsunami source area.

Back-propagation was also applied to primary crests to identify the area of major seafloor uplift in the tsunami source area. However, to avoid incorporating data strongly affected by nonlinear effects or dispersion, it is necessary to limit the input data to near-field tsunami observations in deep water. To achieve this, only the primary crests observed by OBPGs and GPS buoys were used for this back-propagation.

All of the back-propagation curves of primary crests, except those from stations GPS807 and GPS806, pass through an area centered around N38° E143.5° (indicated by the gray dotted line in Fig. 3b), several tens of kilometers east of the epicenter. If the area of seafloor uplift was confined to this small area, most of the primary crest arrival times observed at GPS buoys and OBPGs are reasonably

explained. However, this is but one of several solutions that can explain the observed arrival times of primary crests, as discussed below.

During a great earthquake such as the 2011 Great East Japan earthquake, there may be seismic activity and uplift at multiple locations within the source area. If this is the case, it is difficult to identify the area of maximum uplift by back-propagation of primary crests.

Furthermore, the back-propagation analysis was based on the assumption that tsunami phase velocity is equal to the square root of gravity multiplied by water depth. If the phase velocity is nonlinear, wave crests travel faster than this. On the other hand, dispersion results in wave crests moving more slowly. These effects may cause some estimation errors in areas of large uplift.

It may have been the effect of dispersion that made it difficult to explain the back-propagation curves from stations GPS807 and GPS806 (Fig. 3); otherwise, the area of seafloor uplift may have extended farther in the north–south direction, rather than occurring only to the east of the epicenter.

MODEL-3: TSUNAMI WAVEFORM INVERSION

Tsunami waveform inversion is a technique that applies a least-squares approach to observed tsunami waveforms to identify the tsunami source from the spatial distribution of either fault slip or initial sea-surface displacement. This technique has been applied in many studies of past tsunami events (e.g. Satake 1989; Tanioka et al. 2006; Fujii and Satake 2008; Saito et al. 2010), including the 2011 Great East Japan earthquake (Fujii et al. 2011). Some studies have proposed a tsunami forecasting algorithm based on inversion of offshore tsunami waveforms (Titov et al. 2005; Wei et al. 2008; Tsushima et al. 2009). Here, we summarize the results of tsunami waveform inversion for the 2011 Great East Japan earthquake by Tsushima et al. (2011).

The tsunami was recorded at several offshore tsunami stations (Fig. 2). Waveforms recorded at offshore stations provide a tsunami source signature without distortions from complex coastal topography (González et al. 2005). To take advantage of these undistorted signals, Tsushima et al. (2011) chose to use tsunami waveform data recorded at only four OBPGs (Hirata et al. 2002, Kanazawa and Hasegawa 1997) and five GPS buoys (Kato et al. 2005). Their inversion included the impulsive tsunami waveforms that were recorded at OBPG stations TM1 and TM2 and GPS buoys 802 and 804 (Figs. 4a and 4b). The model derived from those data explains a source of impulsive tsunami.

The modeled distribution of initial sea-surface displacement indicates the tsunami source area. The inversion method applied by Tsushima et al. (2011) is part of a tsunami forecasting algorithm developed by Tsushima et al. (2009). In this inversion, two constraints are imposed to stabilize the solution of the inverse problem: a smoothing constraint and a damping constraint. The damping constraint is based on the presumption that the initial sea-surface displacement due to a tsunamigenic earthquake will be zero at locations distant from the epicenter. Green’s functions were computed by finite-difference approximation of linear long-wave equations (Satake 1995).

The observed and modeled tsunami waveforms matched well (Figs. 4a and 4b), and the modeled uplift occurred in a roughly circular area between the epicenter and the trench (Fig. 4c). Determination of a more accurate location and extent of the source area of the impulsive tsunami could not be achieved because of insufficient azimuthal coverage of the offshore stations included in the inversion (Tsushima et al. 2011); nonetheless, the inversion results indicate that the intense tsunami was caused by considerable sea-surface elevation near the trench.

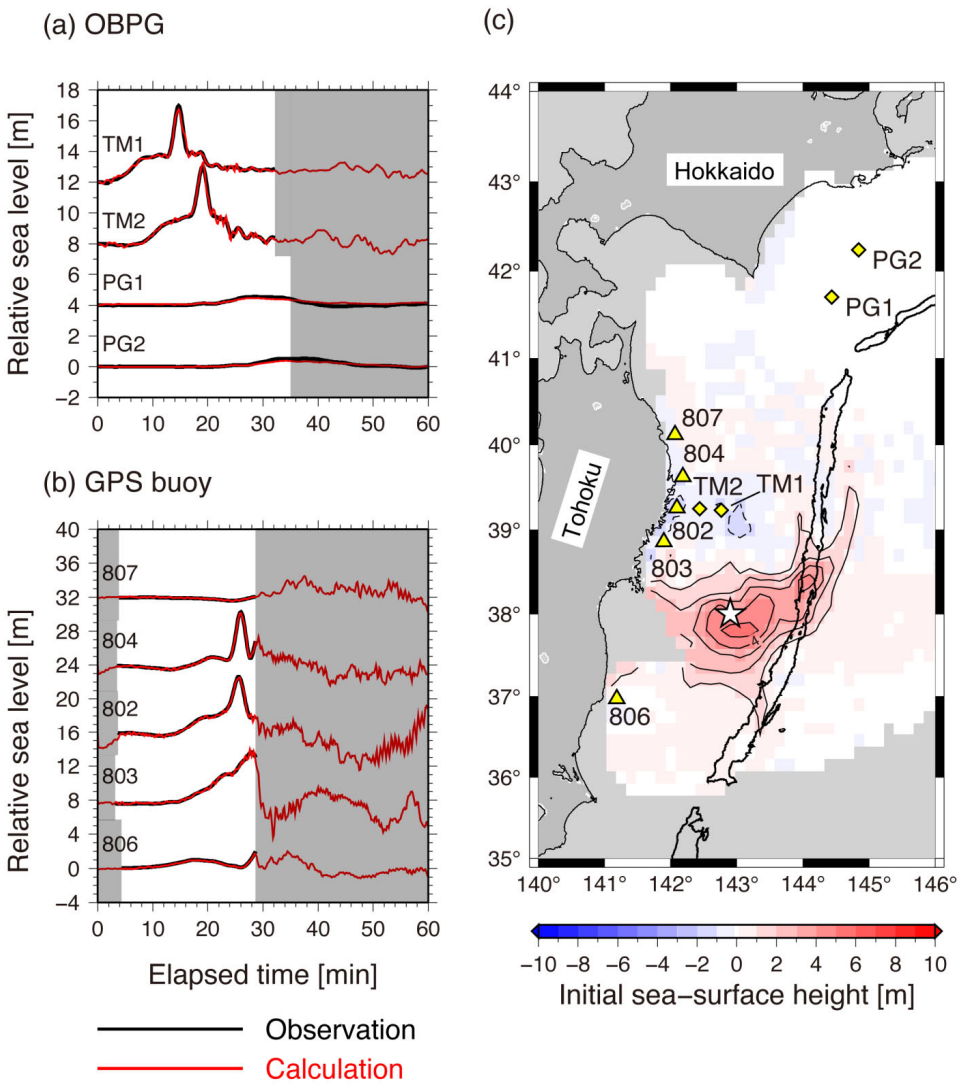

Fig. 4 Result of tsunami waveform inversion by Tsushima et al. (2011) using selected offshore tsunami waveforms from the 2011 Great East Japan earthquake. Comparison of observed (black lines) and modeled (red lines) waveforms at (a) four OBPGs and (b) five GPS buoys. Only the waveforms in unshaded areas of each panel were included in the inversion. (c) Distribution of modeled initial sea-surface elevation. Star indicates epicenter used as the damping constraint in the inversion. Areas shaded gray are outside the influence area. Contour interval is 1 m.

DISCUSSION

The strong impulsive tsunami waves of the 2011 Great East Japan earthquake are represented by the primary crests recorded at offshore observation stations off the Pacific coast of the Tohoku district (Fig. 2). Tsunami waveform inversion (MODEL-3) of selected data (that were not distorted by coastal topography) from offshore stations showed considerable sea-surface elevation in the region between the epicenter and the Japan Trench (Fig. 4c). The arrival times of primary crests at most offshore stations are consistent with an area of maximum uplift between the epicenter and the trench (Fig. 3b). Furthermore, the area of large slip obtained by inversion of seismic strong-motion waves (Fig. 1b) is almost coincident with the source area determined by back-propagation (Fig. 3b) and the area of sea-level uplift determined by tsunami waveform inversion (Fig. 4b). Therefore, we conclude that the

source of the initial impulsive tsunami was probably within the area between the epicenter and the Japan Trench.

Data used in MODEL-1 were regional strong-motion data recorded on land over several minutes starting from the first seismic activity of the 2011 Great East Japan earthquake. Data used in MODEL-3 were tsunami waveform data recorded at offshore observation stations during the 35-min period following the main shock. Application of these modeling methods to data from the 2011 Great East Japan earthquake suggests that both have the potential to provide forewarning of an intense tsunami generated by a near-field large earthquake, provided that there is sufficient processing and analysis time.

Tsunami back-propagation using selected near-field offshore data showed that the method of MODEL-2 may be able to provide forewarning of an intense tsunami generated by a large near-field earthquake, provided that real-time data transmission is available. For MODEL-2, individual back-propagations were initially performed based on initial tsunami arrival times (Fig. 3a) and on primary crest arrival times (Fig. 3b) at offshore observation stations; both inversions included

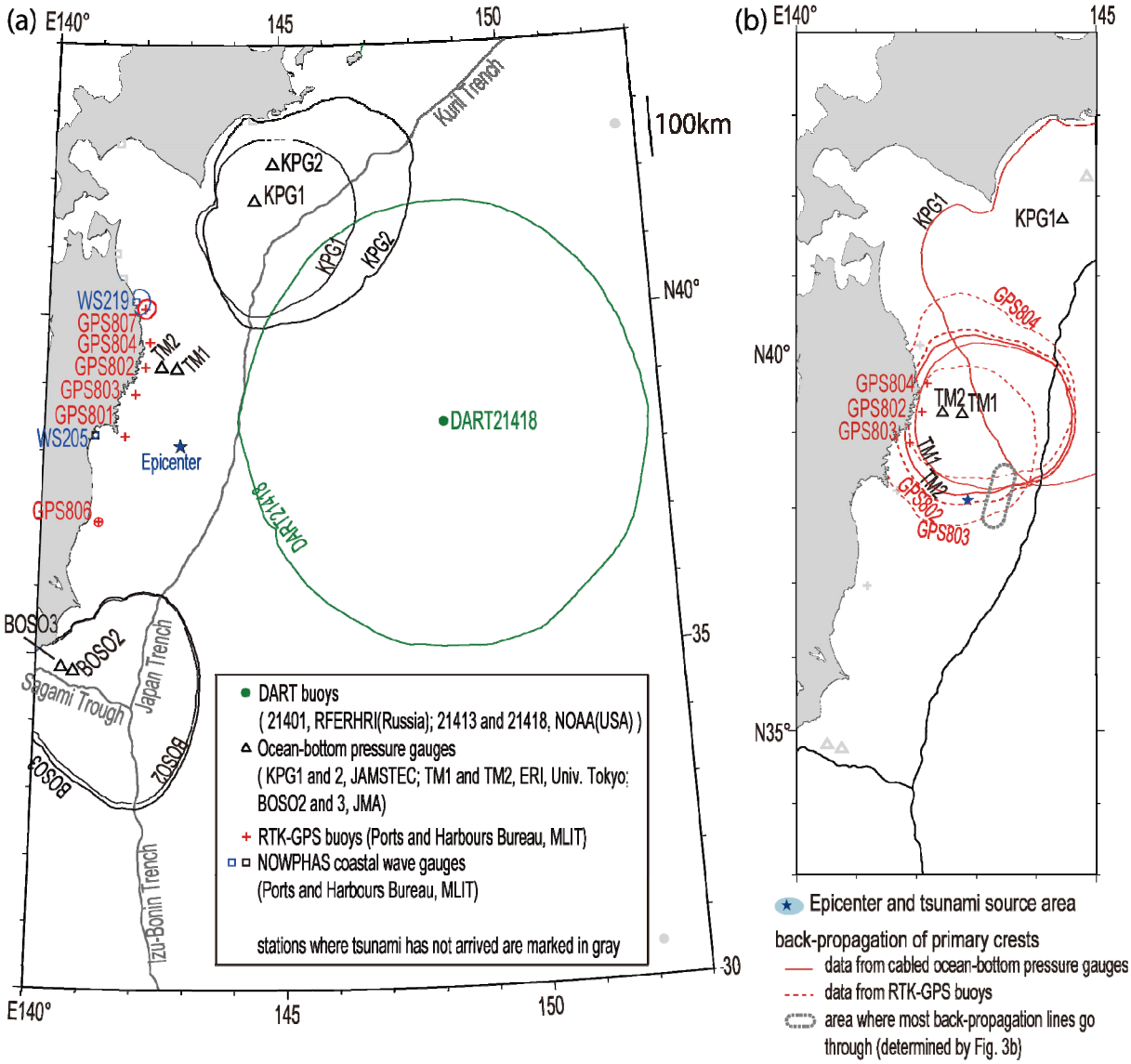

Fig. 5 Tests of rapid determination based on initial 30 min of data at offshore observation stations: (a) tsunami source area determined by back-propagation of tsunami arrivals and (b) intense tsunami source determined from occurrence times of primary tsunami crests.

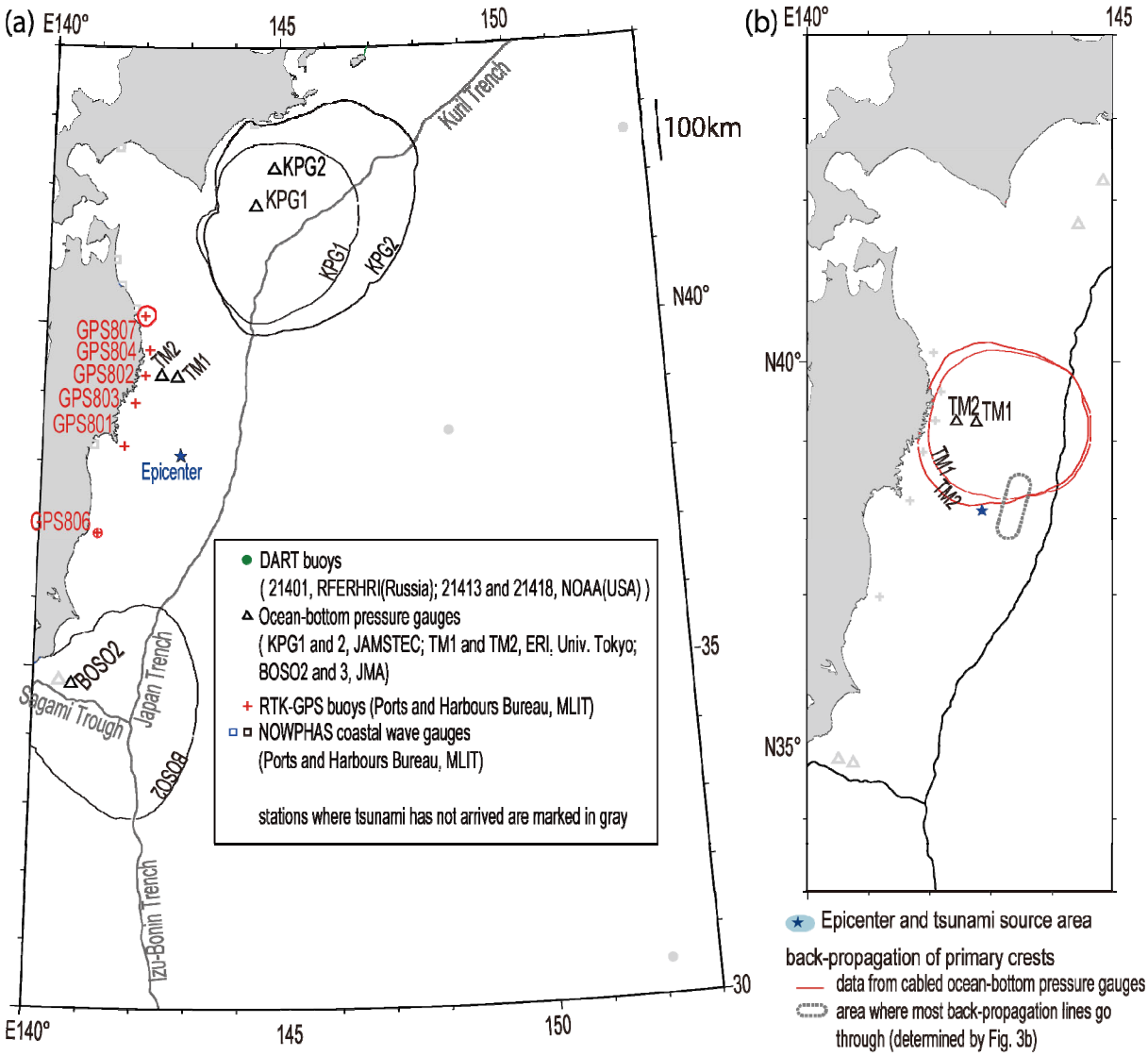

Fig. 6 Tests of rapid determination based on initial 20 min of data at offshore observation stations: (a) tsunami source area determined by back-propagation of tsunami arrivals and (b) intense tsunami source determined from occurrence times of primary tsunami crests.

waveform data recorded more than 30 min after the main shock. However, when input data were limited to those recorded within 30 min of the main shock (Fig. 5a and 5b), the source area of the intense tsunami was only slightly east of that determined from longer wave trains (Fig. 5b). The data recorded within 20 min of the main shock (Fig. 6) were insufficient to determine the location of the source of the intense tsunami.

However, if the back-propagation analyses of Figs 5a and 6a had been applied in real time, the tsunami arrival-time data recorded within 20–30 min after the main shock may have provided important information on the extent of the greate tsunami source area. Back-propagation analysis using the 30-min dataset (Fig. 5a) estimated a tsunami source area that was both wider than 180 km and longer than 480 km. The boundaries of the tsunami source area so defined by back-propagation of DART buoy 21418, GPS buoys along the coastline, and OBPGs KPG2 and BOSO3. And, the epicenter and the stations where sea-level changes were almost synchronous with the arrival of seismic wave (TM1, TM2, GPS801, GPS802, GPS803, and GPS 804) must be within the tsunami source area. Similarly, back-propagation analysis using the 20 min dataset indicated a wider than 130 km and

longer than 480 km. From tsunami data obtained in the Pacific Ocean around Japan, Abe (1975) empirically derived the following relationships:

$$M_0 = 1.23 \times 10^6 S^{3/2}, \quad S = 0.8 S_t, \tag{1}$$

where M_0, S, and S_t are seismic moment (Nm), rectangular area (m^2) of the seismic fault, and rectangular area (m^2) of the tsunami source, respectively.

Kanamori (1977) used worldwide earthquake data to establish the following relationship between seismic moment M_0 and moment magnitude M_w:

$$\log_{10} M_0 = 1.5 M_W + 9.1. \tag{2}$$

Applying Eqs. (1) and (2) to the 20- and 30-min datasets gives M_w values of ≥8.7 and ≥8.8, respectively, slightly lower than the final moment magnitude provided by the JMA earthquake catalogue (M_w 9.0).

CONCLUSIONS

Based on our comparison of models derived independently by (1) strong ground motion waveform inversion, (2) back-propagation of tsunami arrival times at offshore observation stations, and (3) tsunami waveform inversion, we concluded that the origin of the destructive impulsive tsunami that struck the Pacific coast of Tohoku after the 2011 Great East Japan earthquake probably formed between the epicenter and the Japan Trench.

Each of the above methods can be applied in real time, and each would have detected the source of the intense tsunami from either seismic or tsunami waveform data within about 35 min of the main shock. Furthermore, seismic waveform inversion or tsunami waveform inversion would have determined a reasonably accurate seismic magnitude of this mega-earthquake within about 20 min of the main shock.

We thus conclude that individual real-time application of each of the above methods could detect intense tsunami sources and approximate seismic magnitudes of future large earthquakes in the Japan region. Furthermore, we expect that these models used in combination would improve our ability to provide timely warnings of impending tsunamis.

ACKNOWLEDGEMENTS

This work was partly supported by the Science and Technology Research Partnership for Sustainable Development (SATREPS) Research Project on Enhancement of Technology to Develop Tsunami-resilient Community, promoted by the Japan Science and Technology Agency (JST) and Japan International Cooperation Agency (JICA). Tsunami waveform data were acquired from the Port and Harbour Bureau of the Ministry of Land, Infrastructure, Transport and Tourism (MLIT); the Japan Agency for Marine-Earth Science and Technology (JAMSTEC); the Earthquake Research Institute (ERI) at Tokyo University; the Japan Meteorological Agency (JMA); the Russian Far Eastern Regional Hydrometeorological Research Institute (RFERHRI); and the United States National Oceanic and Atmospheric Administration (NOAA). We used Generic Mapping Tools software (Wessel and Smith 1998) to prepare our figures.

REFERENCES

Abe, K. (1975). “Reliable estimation of the seismic moment of large earthquakes.” *Journal of Physics of the Earth*, Vol. 23, 381-390.

Akaike, H. (1980). “*Likelihood and the Bayes procedure, in Bayesian statics.*” edited by J. M.

Bernardo, M. H. DeGroot, D. V. Lindley, and A. F. M. Smith, University Press, Valencia, Spain.
Amante, C. and B. W. Eakins (2009). "ETOPO1 1 arc-minute global relief model: Procedures, data source and analysis." *NOAA Technical Memorandum*, NESDIS NGDC-24, 19p.
Aoi, S., K. Obara, S. Hori, K. Kasahara, and Y. Okada (2000). "New strong-motion observation network: Kik-net." *EOS, Transactions, American Geophysical Union*, Vol. 81, F863.
Bouchon, M. (1981). "A simple method to calculate Green's functions for elastic layered media." *Bulletin of the Seismological Society of America*, Vol. 71, 959-971.
Fujii, Y., and K. Satake (2008). "Tsunami sources of the November 2006 and January 2007 great Kuril earthquakes." *Bulletin of the Seismological Society of America*, Vol. 98, 1559-1571, doi:10.1785/0120070221.
Fujii, Y., K. Satake, S. Sakai, M. Shinohara, and T. Kanazawa (2011). "Tsunami source of the 2011 off the Pacific coast of Tohoku Earthquake." *Earth, Planets and Space*, Vol. 63, 815-820.
Fujisawa, I., S. Tateyama, and J. Fujisaki (1986). "Permanent ocean-bottom earthquake and tsunami observation system off the Boso Peninsula", *Weather Service Bulletin*, Vol. 53, 127-166. (in Japanese)
Fukahata, Y., Y. Yagi, and M. Matsu'ura (2003). "Waveform inversion for seismic source processes using ABIC with two sorts of prior constraints: comparison between proper and improper formulations." *Geophysical Research Letters*, Vol. 30, 1305, doi:10.1029/2002GL016293.
González, F. I., E. N. Bernard, C. Meinig, M. C. Ebel, H. O. Mofjeld, and S. Stalin (2005). "The NTHMP tsunameter network." *Natural Hazards*, Vol. 35, 25-39, doi:10.1007/s11069-004-2402-4.
Hayashi, Y., H. Tsushima, K. Hirata, K. Kimura, and K. Maeda (2011). "Tsunami source area of the 2011 off the Pacific Coast of Tohoku Earthquake determined from tsunami arrival times at offshore observation station." *Earth, Planets and Space*, Vol. 63, 809-813.
Hirata, K., M. Aoyagi, H. Mikada, K. Kawaguchi, Y. Kaiho, R. Iwase, S. Morita, I. Fujisawa, H. Sugioka, K. Mitsuzawa, K. Suyehiro, H. Kinoshita, and N. Fujiwara (2002). "Real-time geophysical measurements on the deep seafloor using submarine cable in the southern Kurile subduction zone." *IEEE Journal of Oceanic Engineering*, Vol. 27, 170-181.
Hirose, F., K. Miyaoka, N. Hashimoto, T. Yamazaki, and M. Nakamura (2011). "Outline of the 2011 off the Pacific coast of Tohoku Earthquake (Mw 9.0)—Seismicity: foreshocks, mainshock, aftershocks, and induced activity—." *Earth Planets, and Space*, Vol. 63, 513-518.
Hoshiba, M., K. Ohtake, K. Iwakiri, T. Aketagawa, H. Nakamura, and S. Yamamoto (2010). "How precisely can we anticipate seismic intensities? A study of uncertainty of anticipated seismic intensities for the Earthquake Early Warning method in Japan." *Earth Planets, and Space*, Vol. 62, 611-620.
Hoshiba, M., K. Ohtake, K. Iwakiri, T. Aketagawa, H. Nakamura, and S. Yamamoto (2011). "Outline of the 2011 off the Pacific coast of Tohoku earthquake (Mw9.0) – earthquake early warning and observed seismic intensity –." *Earth Planets, and Space*, Vol. 63, 547-551.
Ide, S., M. Takeo, and Y. Yoshida (1996). "Source process of the 1995 Kobe earthquake: Determination of spatio-temporal slip distribution by Bayesian modeling." *Bulletin of the Seismological Society of America*, Vol. 86, 547-566.
Ito, Y., T. Tsuji, Y. Osada, M. Kido, D. Inazu, Y. Hayashi, H. Tsushima, R. Hino, and H. Fujimoto (2011). "Frontal wedge deformation near the source region of the 2011 Tohoku-Oki earthquake." *Geophysical Research Letters*, Vol.38, L00G05, doi:10.1029/2011GL048355.
Japan Meteorological Agency (2011). "*Monthly Report on Earthquakes and Volcanoes in Japan March 2011*." pp.57-148. (in Japanese)
Kanamori, H. (1977). "The energy release in great earthquakes." *Journal of Geophysical Research*, Vol. 82, 2981-2987.
Kanazawa, T., and H. Hasegawa (1997). Ocean-bottom observatory for earthquakes and tsunami off Sanriku, north-east Japan using submarine cable, *International Workshop on Scientific Use of Submarine Cables, Comm. for Sci. Use of Submarine Cables*, Okinawa, Japan, 208-209.
Kato, T., Y. Terada, K. Ito, R. Hattori, T. Abe, T. Miyake, S. Koshimura, and T. Nagai (2005). "Tsunami due to the 2004 September 5th off the Kii Peninsula earthquake, Japan, recorded by a

new GPS buoy", *Earth Planets, and Space*, Vol. 57, 279-301.
Kennett, L. N. and N. J. Kerry (1979). "Seismic waves in a stratified half space." *Geophysical Journal of the Royal Astronomical Society*, Vol. 57, 557-583.
Kinoshita, S. (1998). "Kyoshin net (K-NET)." *Seismological Research Letters*, Vol. 69, 209-332.
Nagai, T., S. Satomi, Y. Terada, T. Kato, K. Nukada, and M. Kudaka (2005). "GPS buoy and 4 seabed installed wave gauge application to offshore tsunami observation", *Proceedings of the 15th International Offshore and Polar Engineering Conference*, Vol. III, 292-299.
Nakayama, W. and M. Takeo (1997). "Slip history of the 1994 Sanriku-haruka-oki, Japan, earthquake deduced from strong-motion data." *Bulletin of the Seismological Society of America*, Vol. 87, 918-931.
Saito, T., K. Satake, and T. Furumura (2010). "Tsunami waveform inversion including dispersive waves: the 2004 earthquake off Kii Peninsula, Japan." *Journal of Geophysical Research*, Vol. 115, B06303, doi:10.1029/2009JB006884.
Satake, K. (1989). "Inversion of tsunami waveforms for the estimation of heterogeneous fault motion of large submarine earthquakes: The 1968 Tokachi-oki and 1983 Japan Sea earthquakes." *Journal of Geophysical Research*, Vol. 94, 5627-5636, doi:10.1029/JB094iB05p05627.
Satake K. (1995). "Linear and nonlinear computations of the 1992 Nicaragua earthquake tsunami." *Pure and Applied Geophysics*, Vol. 144, 455-470, doi:10.1007/BF00874378.
Seno, T. and K. Hirata (2007). "Did the 2004 Sumatra-Andaman earthquake involve a component of tsunami earthquakes?" *Bulletin of the Seismological Society of America*, Vol. 97, S296–S306.
Suzuki, W., S. Aoi, H. Sekiguchi, and T. Kunugi (2011). "Rupture process of the 2011 Tohoku-Oki mega-thrust earthquake (M9.0) inverted from strong-motion data." *Geophysical Research Letters*, Vol. 38, L00G16, doi:10.1029/2011GL049136.
Takeo, M. (1985). "Near-field synthetic seismograms taking into account the effect of an elasticity." *Papers in Meteorology and Geophysics*, Vol. 36, 245-257. (in Japanese)
Tanioka, Y., Yudhicara, T. Kususose, S. Kathiroll, Y. Nishimura, S. Iwasaki, and K. Satake (2006). "Rupture process of the 2004 great Sumatra-Andaman earthquake estimated from tsunami waveforms." *Earth, Planets and Space*, Vol. 58, 203-209.
Titov, V. V., F. I. González, E. N. Bernard, M. C. Eble, H. O. Mojfeld, J. C. Newman, and A. J. Venturato (2005). "Real-time tsunami forecasting: Challenges and solutions." *Natural Hazards*, Vol. 35, 35-41, doi:10.1007/s11069-004-2403-3.
Tsushima, H., R. Hino, H. Fujimoto, Y. Tanioka, and F. Imamura (2009). "Near-field tsunami forecasting from cabled ocean bottom pressure data." *Journal of Geophysical Research*, Vol. 114, B06309, doi:10.1029/2008JB005988.
Tsushima, H., K. Hirata, Y. Hayashi, Y. Tanioka, K. Kimura, S. Sakai, M. Shinohara, T. Kanazawa, R. Hino, and K. Maeda (2011). "Near-field tsunami forecasting using offshore tsunami data from the 2011 off the Pacific coast of Tohoku Earthquake." *Earth, Planets and Space*, Vol. 63, 821-826.
Wei, Y., E. N. Bernard, L. Tang, R. Weiss, V. V. Titov, C. Moore, M. Spillane, M. Hopkins, and U. Kanoglu (2008). "Real-time experimental forecast of the Peruvian tsunami of August 2007 for U.S. coastlines." *Geophysical Research Letters*, Vol. 35, L04609, doi:10.1029/2007GL032250.
Wessel, P., and W. H. F. Smith (1998). "New improved version of Generic Mapping Tools released." *EOS, Transactions, American Geophysical Union*, Vol. 79, 579.
Yoshida, Y., H. Ueno, D. Muto, and S. Aoki (2011). "Source process of the 2011 Off the Pacific Coast of Tohoku Earthquake with the combination of teleseismic and strong motion data." *Earth, Planets and Space*, Vol. 63, 565-569.